

# DEUTSCHES ELEKTRONEN-SYNCHROTRON **DESY**

DESY 77/74  
November 1977



## Results from PLUTO

by

Gerhard Knies

NOTKESTRASSE 85 · 2 HAMBURG 52

To be sure that your preprints are promptly included in the  
**HIGH ENERGY PHYSICS INDEX** ,  
send them to the following address ( if possible by air mail ) :

DESY  
Bibliothek  
2 Hamburg 52  
Notkestieg 1  
Germany

## RESULTS FROM PLUTO

Gerhard Knies  
Deutsches Elektronen-Synchrotron DESY  
Notkestrasse 85, D-2000 Hamburg 52  
Germany

### ABSTRACT

Results obtained by the PLUTO collaboration from the 1976 data taking period at the electron-positron storage ring DORIS are presented. We report results on the total  $e^+e^-$  annihilation cross section, on inclusive measurements, on three new decay modes of the  $J/\psi$ , and on various aspects of the heavy lepton  $\tau$ . Among these there is an upper limit on the  $\tau$  lifetime and the first evidence for the possible decay  $\tau \rightarrow \nu A_1$ .

Invited Talk presented at the International Symposium on Lepton Photon Interactions at High Energies, Hamburg (1977).



INTRODUCTION

In this talk I am going to present results from PLUTO which were gathered from data taken during 1976 at DORIS. In 1977 PLUTO was shut down for an upgrading program. The results are due to the work of the following physicists who were involved in operating the detector and analyzing the data:

- DESY: G. Alexander, J. Burmester, L. Criegee, H.-C. Dehne, K. Derikum, R. Devenish, J.D. Fox, G. Flügge, G. Franke, Ch. Gerke, P. Harms, G. Horlitz, Th. Kahl, G. Knies, M. Rössler, R. Schmitz, U. Timm, H. Wahl, P. Waloschek, G.-C. Winter, S. Wolff, W. Zimmermann

- Aachen: W. Wagner
- Hamburg: V. Blobel, B. Koppitz, E. Lehmann, E. Lohrmann, W. Lührs
- Siegen: A. Bäcker, J. Bürger, C. Grupen, G. Zech
- Wuppertal: H. Meyer, K. Wacker

Furthermore I would like to express my appreciation for the supportive efforts of our technicians, the DORIS operating crew and the computer center staff at DESY.

I will talk on the following topics:

- I The Detector PLUTO
- II Total and Partial Cross Sections for  $e^+e^- \rightarrow$  Hadrons
- III Inclusive Particle Production
- IV New  $J/\psi(3.1)$  Decay Modes
- V Investigations of the Heavy Lepton
- A) Summary of Published Results
- B) Upper Limit to the  $\tau$  Lifetime
- C) Associated  $e\bar{p}\pi^0$  Production and the Decay  $\tau \rightarrow \nu A_1$

I THE DETECTOR PLUTO

I will give a very brief sketch of some basic features of the detector PLUTO. Fig. 1 shows a cross section of the detector together with its most important parameters. PLUTO is a solenoidal magnetic detector with a large solid angle for triggering ( $0.87 \times 4\pi$ ) and for track measurement. The trigger is based on track signals from the proportional chambers. Also I would like to emphasize the following:

- a) the hadron-muon separation achieved by the 68 cm thick iron absorber and the muon chambers;
- b) the separation of electrons from hadrons and muons achieved by lead converters interspaced between the proportional chambers;

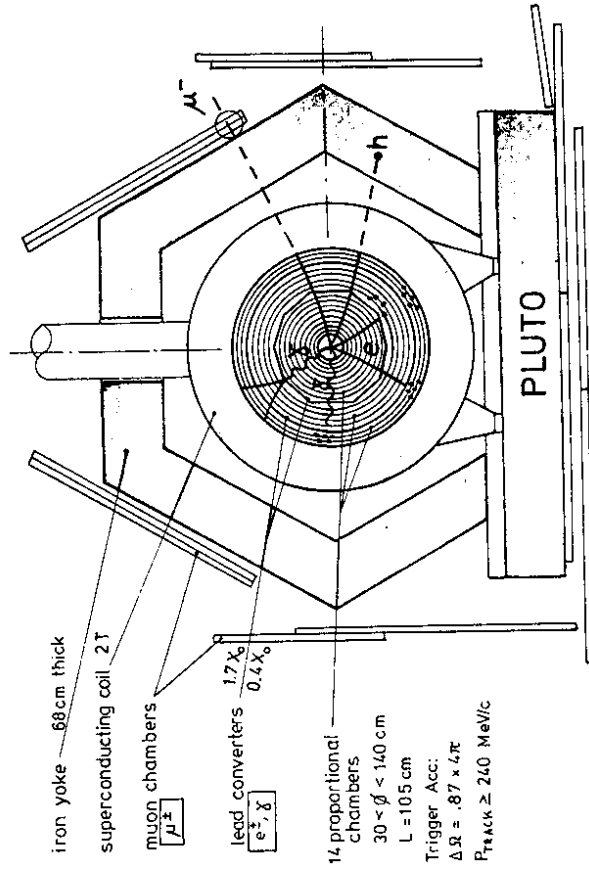


Fig. 1 The PLUTO detector, cross section perpendicular to the beam axis

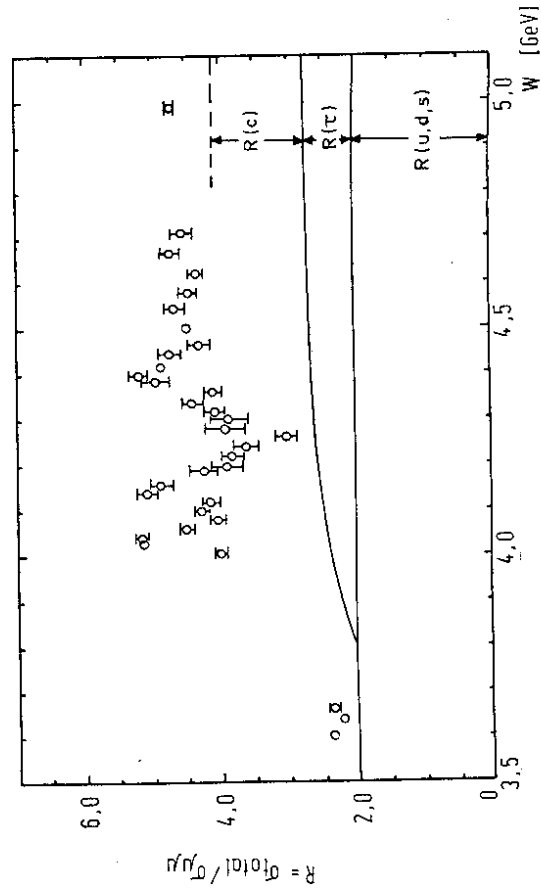


Fig. 2 The total cross section for  $e^+e^- \rightarrow$  hadrons, in units of  $\sigma(e^+e^- \rightarrow \mu^+\mu^-)$

c) the  $\gamma$ -detection and direction measurement obtained by the lead converters and the proportional chambers.

These features furnish some particle identification (electron-muon-hadron-photon) and are very important for the results I am going to present. More details about the detector have been published elsewhere<sup>1</sup>.

## II TOTAL AND PARTIAL CROSS SECTIONS FOR $e^+e^-$ ANNIHILATION

### A. The Method

I very briefly review the most important ingredients of the method<sup>2</sup>:

1) The trigger is sensitive to all events having  $\geq 2$  tracks with the following properties:

- a) production angle  $|\cos\theta| \leq 0.87$
- b) transverse momentum  $p \geq 0.240$  GeV/c
- c) at least 2 tracks with an azimuthal opening angle  $\Delta\phi > 45^\circ$ .

2) Event acceptance: For the total hadronic cross section we use events having at least two acoplanar tracks. For 2-prong events the difference in their azimuthal angles is required to be  $\Delta\phi < 150^\circ$ . This cut removes the bulk of two body QED events which occur with a large cross section. Other QED events (e.g.  $e\bar{e}\gamma$ ) are identified in the later analysis and subtracted. However, final states from QED production of heavy lepton pairs are included in our event sample.

3) The probability for an  $e^+e^-$  annihilation event to successfully pass the trigger conditions, pattern recognition, and event-identifying programs varies between 70 and 78%. The event efficiency depends on the prong multiplicities present at different center of mass energies  $W$ , and has been determined from simulated events. We used a jet model<sup>3</sup>, the parameters of which were adjusted to reproduce the total measured energy, the inclusive prong distribution, the production-angle distribution, and the (charged) prong distribution. The best agreement between the jet model and the experiment was achieved with the following parameters:

- a) jet-axis distribution  $\propto 1 + a \cdot \cos^2\theta$ ,  $a = 1$
- b) average momentum transverse to the jet axis  $\langle p_{\perp} \rangle = 350$  MeV/c
- c) neutral : charged energy = 1 : 1

These parameter values were used at all energies  $W$ . The neutral energy accounts for the energy of neutral particles in the final state, for radiative losses in the initial state, and for an artificial deficiency of charged energy since all tracks are interpreted as pions when calculating

<sup>3</sup> The jet model here serves as a technical means for determining the event efficiency rather than as a physical model to interpret the data.

energies from measured momenta. In each energy interval we determined separately as a further parameter the distribution of charged multiplicities yielding partial cross sections.

4) Corrections for background from beam gas and cosmic rays ( $29 \pm 1\%$  of the signal) and from QED final states ( $1.0 \pm 0.3$  nb) have been determined experimentally.

5) The monitor is a small angle Bhabha detector, at  $130 \pm 22$  mrad, measuring a cross section of  $\sigma_M = R_M \cdot \sigma(e^+e^- \rightarrow \mu^+\mu^-)$  with  $R_M = 65$ .

6) Radiative corrections have been applied.

7) For all of these corrections we estimate a systematic error of  $\pm 10\%$ , the main uncertainties coming from event efficiency (7%) and monitor (5%).

### B. Results

In Fig. 2 we show the total cross section  $\sigma_{tot}$  in terms of  $R = \sigma_{tot}/\sigma(e^+e^- \rightarrow \mu^+\mu^-)$ , as a function of  $W$ , the center of mass energy. There are three points at  $W$  around 3.6 GeV, with  $R = 2.3$ . Between 4 and 4.5 GeV we note peaks at  $W = 4.03, 4.15$  and 4.40 GeV. The dip between the two latter peaks, at  $W = 4.27$ , is remarkably deep. For  $W > 4.5$  GeV the data points show no further structure. At  $W = 5$  GeV we find  $R = 4.7$ . The error bars give the statistical errors.

Figure 2 also summarizes what is expected for  $R$  from various sources. At  $W = 3.6$  GeV the quark model provides  $R(q) = 3 \cdot \int Q_i^2 = 6/3$  from  $u, d$  and  $s$  coloured quarks. At  $W = 5$  GeV, we have  $R(q) = 10/3$  from  $u, d, s$  and  $c$  quarks, and a contribution  $R(\tau) = (3\beta - \beta^3)/2$  from the heavy lepton<sup>3</sup>. These predictions are consistent with our experimental findings. Taken at face value, however, there is an excess of  $\Delta R \sim 0.4$  over the expectations. On the other hand, gluonic corrections<sup>4</sup> to the simple quark model result tend to increase  $R(q)$ . The step just below 4 GeV and the structure between 4 and 4.5 GeV are attributed to charm production. The three peaks between 4.0 and 4.5 GeV can be understood as an interplay of thresholds and form factors for the production of charm-meson pairs<sup>5</sup>. If structures at these energies are due to charm production then, as a consequence, charm production is reduced in the dip area of 4.3 GeV.

For more details on the cross section we show in Fig. 3 a break down into multiplicities of 2, 4 and  $\geq 6$  charged particles. All of these multiplicities show the same gross features as  $\sigma_{tot}$ . The dip at 4.3 GeV and the peak at 4.4 GeV, however, hardly show up in the 4-prongs, Fig. 3b. The reduction in charm production at the 4.3 GeV dip is strongest in 2-prongs, Fig. 3a. In fact, it is interesting to note that the non charm cross section, as seen at  $W = 3.6$ , and heavy lepton contributions seem to be sufficient to make up for the observed 2-prong cross section at this energy.

Comparing our  $\sigma_{tot}$  to other experiments we find detailed agreement with recent results from DASP6 (Fig. 4). There are obvious differences with the SLAC-LBL results<sup>7</sup> (Fig. 5).

### III. INCLUSIVE PARTICLE PRODUCTION

#### A. Introduction

The quark-parton picture of hadrons as it has emerged from electroproduction experiments has consequences for the inclusive production of particles in  $e^+e^-$  annihilation. It predicts scale invariance of the inclusive spectrum

$$\frac{s}{\beta} \frac{d\sigma}{dX_E} = f(X_E), \text{ independent of } s,$$

with  $X_E = E$  (particle) /  $E$  (beam) and  $\beta =$  particle velocity, at sufficiently large  $s$ . It relates, through the quark fragmentation function, the inclusive spectra from electroproduction to  $e^+e^-$  annihilation.

The actual comparison of  $e^+e^-$  annihilation and leptonproduction data is an involved subject<sup>8</sup> which I am not going to enter into here. I will concentrate on presenting the results from PLUTO. We have measured the inclusive production of  $K^0$ -mesons,  $J/\psi$ -mesons,  $\rho^0$ -mesons and stable charged particles ( $\mu, \pi, K$  and  $p$ ). Our results on  $K^0$ - and  $J/\psi$ -mesons are published already<sup>9</sup>. The significance of inclusive  $K$ -production for the charm hypothesis has been discussed in detail in the talk of S. Yamada<sup>12</sup>. Since PLUTO and DASP results agree on this topic I am not going to give further details. Results on stable charged particles and on  $\rho^0$ -mesons are new, and inclusive  $J/\psi$ -production has not been measured elsewhere. Therefore, I will talk on these in some detail.

#### B. Inclusive Spectrum of Stable Charged Particles

The SLAC-LBL<sup>10</sup> and the DASP<sup>11</sup> collaboration have measured the inclusive spectrum of charged particles. Their results do not agree, in particular at large  $X$ -values. Like the SLAC-LBL detector, PLUTO measures the momentum but does not measure the particle mass or energy. We therefore use the fractional momentum  $X_p =$  particle momentum /  $E$  (beam) which relates to  $X_E$  by  $X_p = \beta \cdot X_E$ . In the limit  $\beta = 1$  where scaling should hold  $X_p$  and  $X_E$  are equal. In Fig. 6a we show  $s \cdot d\sigma/dX_p$  vs  $X_p$ . Corrections are made for the small angles not covered by PLUTO. No corrections are applied for radiative losses in the initial state, momentum resolution and contribution from heavy leptons. We note that the inclusive particle spectrum is scale invariant within 20% for  $X_p > 0.5$  and  $W > 3.6$  GeV. Deviations from scaling for  $X_p < 0.5$  are obvious and are attributed to the charm threshold as discussed in the talk of S. Yamada<sup>12</sup>. For  $W > 4.03$  GeV the shape of the inclusive particle spectrum is exponential ( $\propto \exp(-7.7 X_p)$ ) for  $X_p > 0.15$ . In Fig. 6b we compare the PLUTO result (straight line) to the measurements from DASP<sup>11</sup> and SLAC-LBL<sup>10</sup>. We note that the PLUTO result agrees well with the measurements by DASP, a very different detector, and that it differs from what is found by the similar SLAC-LBL detector.

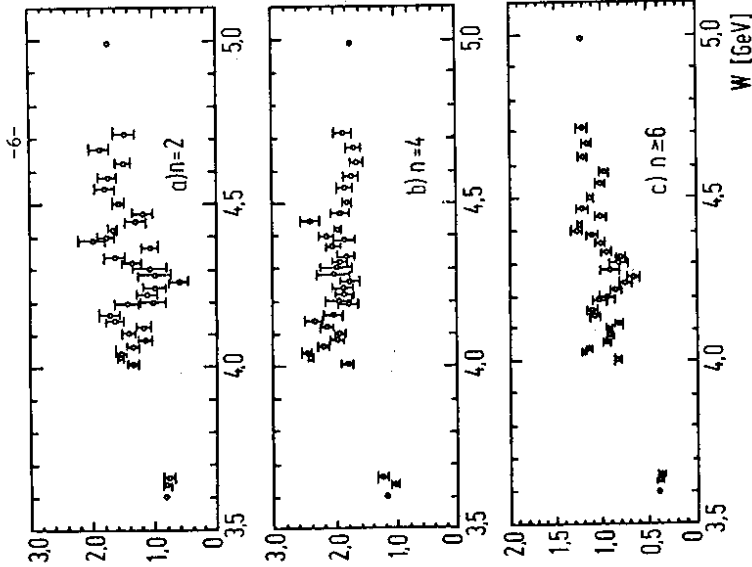


Fig. 3

Breakdown of total cross section ( $R$ ) into charged multiplicities of  $n = 2, 4, \geq 6$

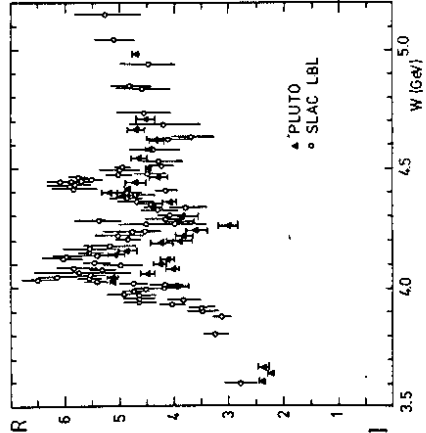


Fig. 5  $\sigma_{tot}(e^+e^- \rightarrow \text{hadrons}) / \sigma_{\mu\mu}$  comparison PLUTO/SLAC-LBL

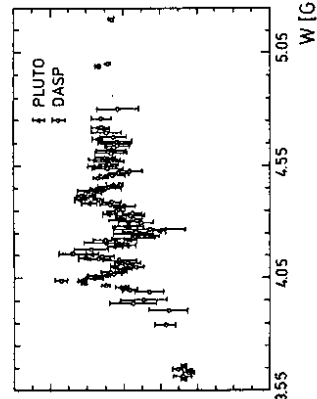


Fig. 4  $\sigma_{tot}(e^+e^- \rightarrow \text{hadrons}) / \sigma_{\mu\mu}$  comparison PLUTO/DASP

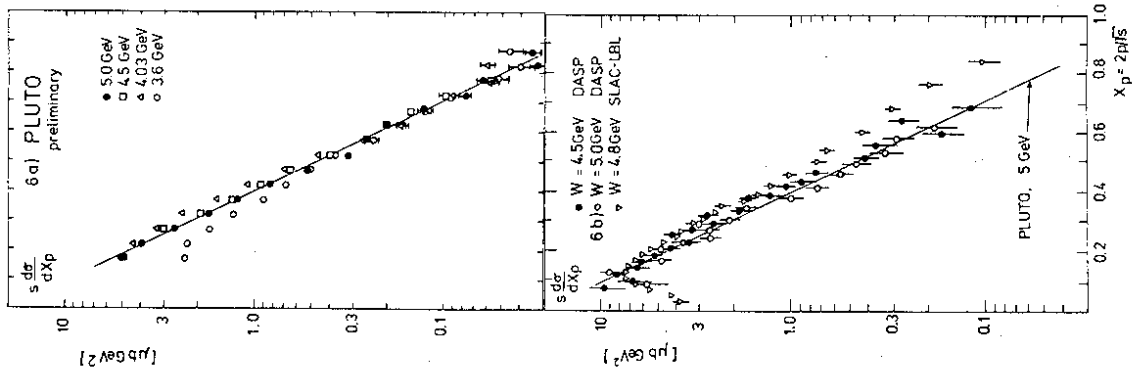


Fig. 6  
 a) PLUTO results  
 b) Comparison with DASP and SLAC-LBL results  
 Systematic errors not included

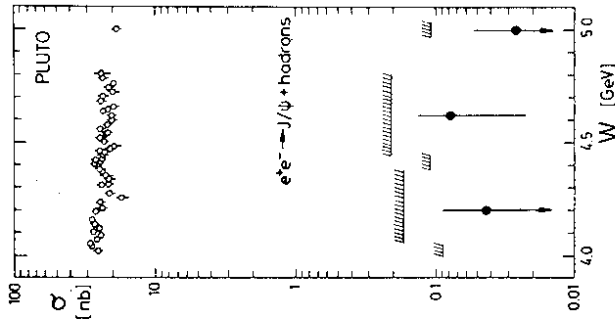


Fig. 7  
 Inclusive cross section for  $e^+e^- \rightarrow J/\psi + \text{hadrons}$   
 For comparison, the total cross section is also shown

Fig. 6  
 a) PLUTO results  
 b) Comparison with DASP and SLAC-LBL results  
 Systematic errors not included

C. Inclusive  $J/\psi$ -Production

This process is relevant for the hypothesis of charm molecules ( $cc\bar{q}\bar{q}$ -systems) which has been invoked<sup>13</sup> to interpret the peaks in  $\sigma_{\text{tot}}$  just above charm threshold (see Fig. 2). In some of these models the formation of such molecules should lead to copious  $J/\psi$ -production, on the order of 10 % of these peaks. After removing radiative  $J/\psi$ -production we find 4 events of the type  $e^+e^- \rightarrow J/\psi + \text{hadrons}$ . Our cross section is shown in Fig. 7. These 4 events correspond to a level of  $\sim 0.1\%$  of  $\sigma_{\text{tot}}$  which is consistent with what is expected<sup>14</sup> from Okubo-Zweig-Lizuka (OZI)-rule<sup>15</sup> violation, but is clearly lower than the above mentioned copious production by molecules.

D. Inclusive  $\rho^0$ -Production

To investigate  $\rho^0$ -production we have assigned pion masses to all tracks and then calculated the invariant mass of all  $\pi^+\pi^-$  combinations. In Fig. 8a we show the resulting invariant mass distribution (upper histogram). At the  $\rho$ -mass there is a broad shoulder. The lower histogram is obtained by combining tracks from different events. Subtracting this uncorrelated and smooth spectrum as a background, the  $\rho$  shows up as a clear signal in Fig. 8b. The two other peaks are from  $K^0$ - and  $\omega$ -decays, and from photon conversions in the beam pipe. The mass spectrum of Fig. 8a has been fitted to a  $\rho^0$ -resonance, a smooth background, and a possible reflection from  $K^*(890)$  production, which centers at the left  $\rho$ -tail, when interpreted as a  $\pi\pi$ -system.

Preliminary results for inclusive  $\rho^0$ -production are shown in Figs. 9 and 10. In Fig. 9 the inclusive  $\rho^0$ -spectrum for  $W > 4.3$  GeV is shown as a function of  $X_E$ . The striking feature is that within its errors, it follows the same exponential shape as found for charged pions<sup>11</sup>, but the absolute value of the  $\rho^0$ -cross section is higher by a factor of 2 - 2.5. Fig. 10 shows the inclusive  $\rho^0$ -cross section at various energies. The systematic uncertainties (mainly from different treatments of the background in the fits) are independent of the energy. We, therefore, see an indication of a step at  $W \sim 4$  GeV, the threshold of charm and heavy lepton production. The average value of  $R(\rho^0) \approx 1.3$  (for  $W > 4$  GeV) may be used for a rough estimate of the fraction of charged pions coming from vector mesons. Assuming  $R(\rho^+) = R(\rho^-) = R(\rho^0)$  and  $R(\omega) = R(\rho^0)$  we find  $R(\pi^+ \text{ from VM}) = 5.8 \cdot R(\rho^0) \approx 7.5$ . Subtracting from the average track multiplicity  $n$ , or from  $R(\text{track}) = n \cdot R = 19$  the known charged  $K$ -rate<sup>11</sup> ( $R(K^+) \approx 2.5$ ), and those pions from  $K_S^0$ -decay<sup>9</sup> ( $R(\pi^+) = \frac{2}{3} R(K^+)$ ), and keeping in mind that there are muons, electrons and protons included in  $R(\text{track})$ , then it is safe to say that  $> 50\%$  of all pions originate from vector-meson decays.

Dominance of vector-meson production over pseudoscalar mesons is expected from the quark model on the basis of spin-state counting.

IV NEW  $J/\psi$  DECAY MODES

A. Introduction

The  $J/\psi$  is considered to be a  $cc$  bound state. If the OZI rule<sup>15</sup>, which forbids strong transitions involving disconnected quark



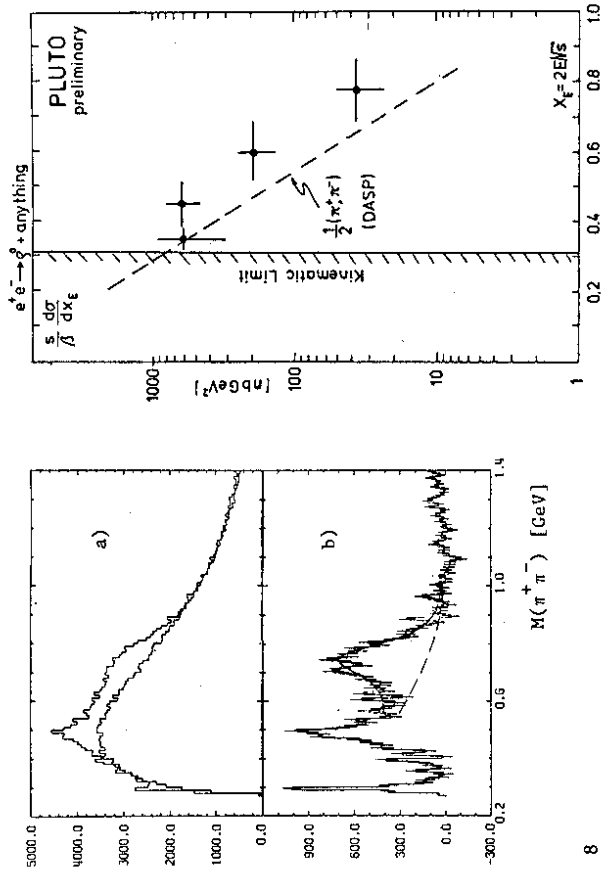


Fig. 8

- a)  $M(\pi^+\pi^-)$  for  $e^+e^- \rightarrow \pi^+\pi^- + \text{anything}$ , upper histogram. The lower histogram shows uncorrelated  $\pi^+\pi^-$  pairs from different events.
- b) Difference between correlated and uncorrelated  $\pi^+\pi^-$  pairs.

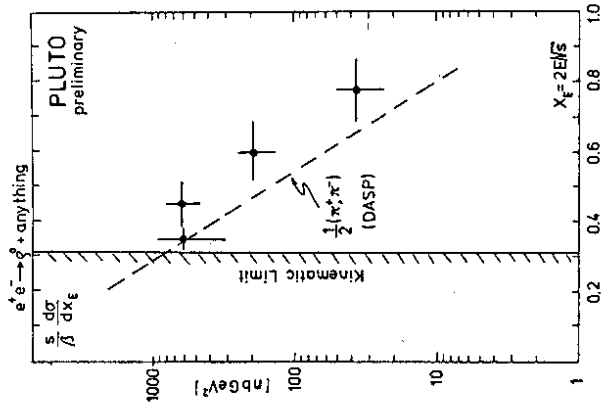


Fig. 9  $\rho^0$  inclusive spectrum for  $4.3 \leq W \leq 5$  GeV.

The dashed line is the average of  $\pi^+$  and  $\pi^-$  inclusive spectrum as measured by DASP.

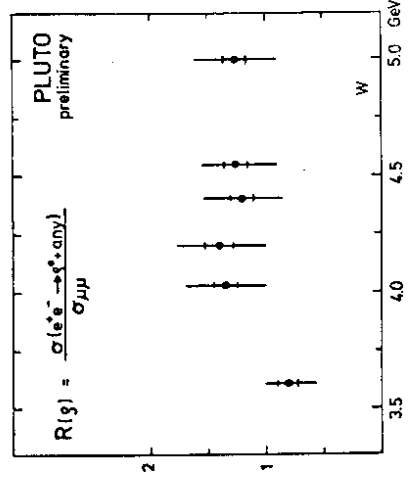


Fig. 10 Inclusive  $\rho^0$  cross section at different CMS energies  $W$ . The larger error bars include systematic uncertainties.

lines, was exact, no strong decays of the  $J/\psi$ -resonance would occur. However, it is known that only 1/3 of the  $J/\psi$ -decays can be attributed to electromagnetic transitions through a virtual photon, leaving  $\approx 2/3$  of the decays to OZI violating strong transitions to non charmed particles. Such strong transitions establish a mixing of  $cc$  and  $qq$   $SU(3)$  states. The relatively large decay rates  $J/\psi \rightarrow \gamma\eta$  ( $0.088 \pm 0.019\%$ ) and  $J/\psi \rightarrow \gamma\eta'$  ( $0.24 \pm 0.06\%$ ) can be accounted for by introducing a  $cc$  component<sup>17</sup> into the  $\eta$  and  $\eta'$  quark wave function. If  $cc$  mixes with  $qq$  in the pseudoscalar  $SU(3)$  multiplet, is there also a mixing in the other well established multiplets like the vector multiplet ( $\omega, \phi$ ) and the tensor multiplet ( $f, f'$ )? The following three decay modes, recently discovered by PLUTO, provide experimental information relating to this question:

mode	branching fraction (%)
$\pi^+\pi^-B$	$0.28 \pm 0.07$
$f\omega$	$0.40 \pm 0.16$
$f\gamma$	$0.20 \pm 0.07$

B.  $J/\psi \rightarrow \omega f, B\pi$

These two decay modes have been observed<sup>18a</sup> in the final state  $\pi^+\pi^-\pi^+\pi^-$ . Fig. 11a shows the  $\pi^+\pi^-\pi^+\pi^-$  mass distribution with an  $\omega$  peak. In Fig. 11b the invariant mass of  $\pi^+\pi^-$  recoiling against the  $\omega$  is plotted. A clear  $f$ -peak shows the decay  $J/\psi \rightarrow \omega f$ .

In Fig. 11c the  $\omega\pi^{\pm}$  mass distribution shows a clear  $B$ -peak, establishing the decay  $J/\psi \rightarrow \pi B$ . Both of these decays are suggestive for a transition  $cc \rightarrow qq$  in the physical  $J^{PC} = 1^{--}$  states, or a mixing between  $J/\psi$  and  $\omega$ , as indicated in the following diagrams:

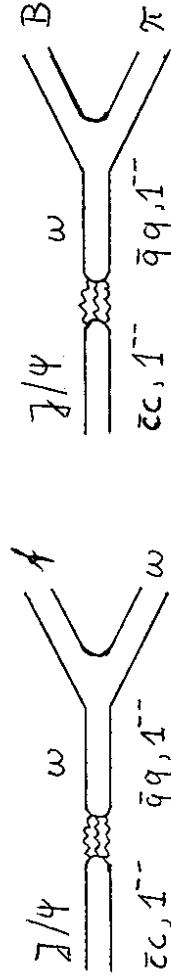


diagram 1

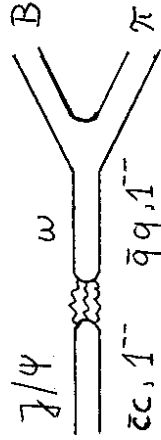


diagram 2

The OZI rule violating transition  $J/\psi \rightarrow \omega$  may also explain the large decay rate  $J/\psi \rightarrow \rho\pi$  ( $BR \approx 1.1\%$ ).

C.  $J/\psi \rightarrow f\gamma$

In Fig. 12 the  $\pi^+\pi^-$  mass spectrum is shown from the final states  $\pi^+\pi^-\pi^+\pi^-$  and  $\pi^+\pi^-\gamma$ . There are peaks at the  $\rho$ -mass and at the  $f$ -mass. We combine these

two channels since experimentally a  $\pi^0$  cannot always be separated from a single photon. From C-parity it is clear that the  $\rho^0$  is associated with a  $\pi^0$ , and the  $f$  with a  $\gamma$ . The assignment of the mass peak at 1.25 GeV to the  $f$ -meson is supported by further experimental tests<sup>18b</sup>. The  $f\gamma$  rate exceeds what we would expect from the above mentioned  $f\omega$  rate using vector-meson dominance model (VDM) for the  $\omega \rightarrow \gamma$  transition (see diagram 3), by about 2 orders of magnitude. The situation here is similar to the observed  $\eta\pi$  and  $\eta\pi'$  rates which are much larger than the expectations based on the pV rate, VDM for  $\rho \rightarrow \gamma$  and SU(3) connecting  $\pi$  with  $\eta$  and  $\eta'$ . A possible mixing scheme to explain the  $f\gamma$  rate is indicated in diagram 4.

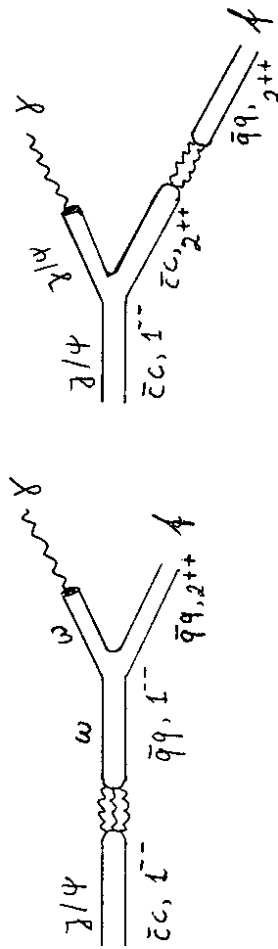


diagram 3

diagram 4

There we have a 2 gluon annihilation connecting  $c\bar{c}$  and  $q\bar{q}$  in the  $2^{++}$  state rather than the 3 gluons which are required for an annihilation process in a  $1^-$  state, as for example in diagram 3. Since diagram 4 is 2 orders lower in the quark-gluon coupling constant it may explain the larger decay rate.

V INVESTIGATIONS OF THE HEAVY LEPTON  $\tau$

Since the first observation of  $e\mu$  events in  $e^+e^-$  annihilation at SPEAR<sup>19</sup> there has been increasing evidence for the existence of a new sequential heavy lepton<sup>20</sup>. This evidence has been frequently reviewed at recent conferences<sup>21</sup>. Here I want to give a brief summary of those results by PLUTO which are already published<sup>22</sup> (subsection A), and describe in more detail two new results, an upper limit on the  $\tau$ -lifetime (B), and first evidence for the possible decay  $\tau \rightarrow A_1 \nu$  (C).

A. Summary of Published Results

These are results from an analysis of events with muons. Since the method and the results have been described already I will limit myself to a very brief summary. However, due to improvements in subtracting QED background, the results have changed a little.

- 1) To begin with I want to say a few words on the method.  $\mu$ -hadron separation is possible with PLUTO for particles with momenta  $p > 1 \text{ GeV}/c$  over a solid angle of  $\Delta\Omega = 0.43 \cdot 4\pi$ . The punch through ( $h \rightarrow \mu$ ) is  $(2.8 \pm 0.7) \%$ . Events require 1  $\mu$ -track plus  $> 1$  further track with  $p > 0.240 \text{ GeV}/c$  and  $|\cos\theta| < 0.87$ . We have dealt with the following backgrounds:

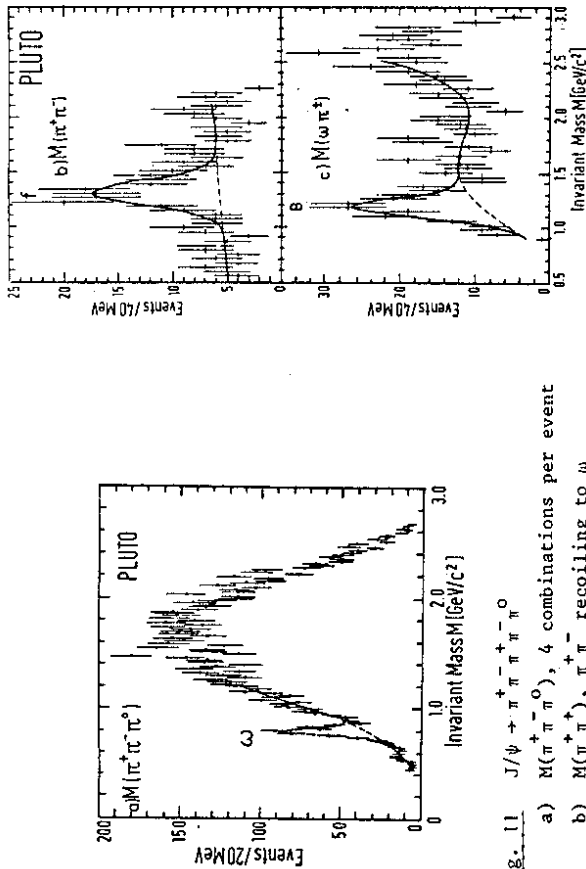


Fig. 11  $J/\psi \rightarrow \pi^+ \pi^- \pi^+ \pi^-$   
 a)  $M(\pi^+ \pi^- \pi^+ \pi^-)$ , 4 combinations per event  
 b)  $M(\pi^+ \pi^- \pi^+)$ ,  $\pi^-$  recoiling to  $\omega$   
 c)  $M(\omega \pi^+)$

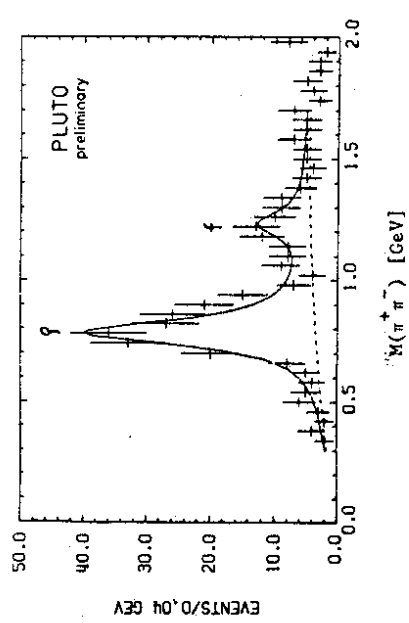


Fig. 12  $J/\psi \rightarrow \pi^+ \pi^- \pi^0$  and  $\pi^+ \pi^- \gamma$

We note that V-A is slightly favoured over V+A, but both are acceptable. Furthermore we have the following results:

- a) Upper limit on the neutrino mass (90 % c.l.) :  
 $M(\nu) < .46 \text{ GeV}$  ( $M(\tau) = 1.93$ )  
 $.54 \text{ GeV}$  ( $M(\tau) = \text{free}$ )

b) Spin assignment: Spin 1/2 does agree with various aspects of the data like the energy dependence of the cross section, total  $\tau$  cross section being consistent with observed decay rates and predicted branching ratios<sup>24</sup> and the  $\mu$ -momentum spectrum consistent with the 3-body decay  $\tau \rightarrow \mu\nu\nu$ . In case of a point like spin 0 particle the total cross section is  $\sigma = 1/4 \cdot \beta^3 \cdot \sigma_{\mu\mu}$ , which is much lower than for spin 1/2 particles ( $\sigma_{\mu\mu}$ ). In this case our  $\mu\mu$  measured muon-cross section requires an unreasonably large branching ratio ( $\approx 100\%$ ) for decay into muons. We therefore rule out spin 0.

- c) In 4-prong events with one muon we find 7 events consistent with

$$\tau\bar{\tau} \rightarrow (\mu^+\nu\nu) + (\rho^0\pi^+\nu)$$

Even though the invariant  $3\mu$  mass is consistent with the  $A_1$  mass, the statistical significance is too poor for any further conclusions. It will come back to this question in subsection C.

B. Upper Limit to the Lifetime

From the 2-prong sample with  $\mu$ -tracks we selected a subsample of 138 events by using additional cuts which remove the main background sources almost entirely. This sample of events we consider as an almost clean  $\tau$ -sample that allows us to infer an upper limit on the  $\tau$ -lifetime.

- 1) The method: Since we are observing just one decay track from each  $\tau$  we cannot measure the decay point directly by intersecting decay tracks. However, the minimum radial distance  $r_{\min}$  of a track from the central beam axis is sensitive to a finite decay length  $l_d$ , as indicated in Fig. 15. The width of the  $r_{\min}$  distribution is already affected by uncertainties in reconstructing tracks (spatial resolution of the detector and multiple scattering) and the finite beam cross section. The finite decay length tends to broaden this distribution further. We have therefore simulated various 1-prong decay modes in PLUTO, folding in the experimental resolution and various decay lengths  $l_d$  of the  $\tau$ . This way we find an (2 s.d.) upper limit of 2 mm for  $l_d$  to be consistent with the events. In our experiment this corresponds to an upper limit for the  $\tau$ -lifetime of

$$\tau_{\tau} \leq 1 \cdot 10^{-11} \text{ s} \quad (95 \% \text{ c.l.})$$

This result is well consistent with the prediction of the standard model of  $\tau = 3 \cdot 10^{-13}$  for  $m_{\tau} = 1.85 \text{ GeV}$ <sup>24</sup>. However, in models where the charged heavy lepton  $\tau$  does not decay into its 'own' neutrino ( $\tau \rightarrow \nu_{\mu}\nu_{\mu}\mu$

$$\left. \begin{array}{l} e^+e^- \rightarrow \mu^+\mu^- \\ e^+e^- \rightarrow \mu^+\mu^-\gamma \\ \gamma\psi'(3.7) \end{array} \right\} \text{ removed by kinematic cuts}$$

$$\left. \begin{array}{l} e^+e^- \rightarrow \mu^+\mu^-\gamma \\ \mu^+\mu^-\gamma \end{array} \right\} \text{ calculated}^{23} \text{ and subtracted}$$

$h \rightarrow \mu$  punch through has been determined experimentally and subtracted

2) Results: We find  $\mu$ -signals in 2-prong and  $> 3$ -prong events. In both of these channels the  $\mu$ -momentum spectrum (Fig. 13) and the energy dependence of the cross section (Fig. 14) are consistent with the production through a pair of heavy leptons:



We therefore expect to see the process

$$e^+e^- \rightarrow \tau^+\tau^- \rightarrow e^+\nu\nu + \mu^+\nu\nu$$

which has the final state signature

$$\mu^+e^+ \text{ 'nothing else' } + \text{ large missing mass.}$$

In fact we find 23 events, where less than 2 may come from punch through. The particular significance of these events for the heavy lepton hypothesis is that they are inconsistent with any charm explanation.

All these data can be consistently interpreted by the production and decay of heavy lepton pairs, using the parameters listed in the following table and assuming a V-A or a V+A structure for the  $\tau \rightarrow \mu\nu\nu$  decay, and

$$\text{using } \sigma_{\tau\tau} = \frac{3\beta - \beta^3}{2} \sigma_{\mu\mu} \text{ and } M(\nu_{\tau}) = 0.$$

Parameters	V - A	V + A
BR( $\tau \rightarrow \mu\nu\nu$ ) [%]	$14 \pm 3.4$	$17 \pm 5$
BR( $\tau \rightarrow 1 \text{ prong}$ ) [%]	$69 \pm 14$	$68 \pm 15$
BR( $\tau \rightarrow e\nu\nu$ ) [%]	$16 \pm 6$	$13 \pm 5$
Mass $M_{\tau}$ [GeV]	$1.93 \pm .05$	$1.82 \pm .08$
$\chi^2/\text{ND}$	$7.5/8$	$11.7/8$

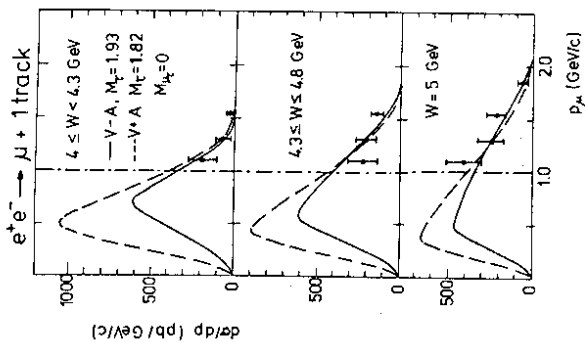


Fig. 13 Muon momentum spectrum for 2-prong events at different energies  $W$ . Curves are from the fits described in the text.

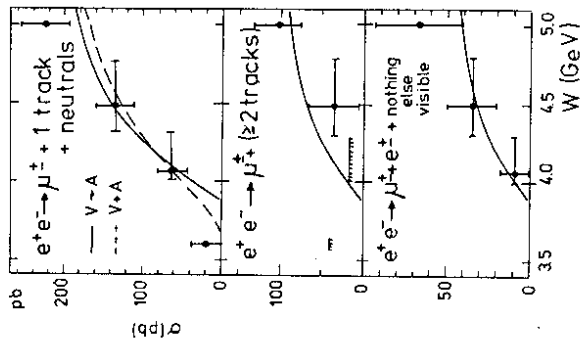


Fig. 14 Cross section  $\sigma$  (pb) for  $P_\mu > 1$  GeV/c. Curves as in Fig. 13.

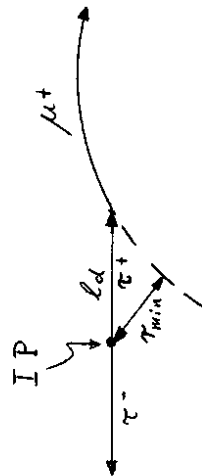


Fig. 15 Definition of  $x_{min}$ . Here the decay  $\tau^+ \rightarrow \mu^+ \nu_\tau$  after a decay length of  $l_d$ , leads to a  $\mu^+$ -track bypassing the interaction point (IP) at a

for example), lifetimes are longer and our upper limit becomes relevant. For a discussion of this subject I refer to the talk of T. Walsh<sup>25</sup> at this conference.

C. Associated  $e^+e^- \pi^0$  Production and the Decay  $\tau \rightarrow \nu A$

This is the first experimental evidence for the possible decay

$$\tau \rightarrow \nu A, \quad (1)$$

which has been predicted by several authors<sup>24</sup>. Let me describe to you briefly the experimental method and also present the discussion of the evidence before giving the results on cross section and branching ratio.

1) Here we used an electron-hadron separation based on a very detailed analysis of the shower pattern induced by a track in the 2-chambers behind the second lead converter. Details of this method will be published elsewhere. The important figures from this method of hadron-electron separation are:

- a) punch through  $P(h \rightarrow e) = 1.2 \%$ ,
- b) efficiency for electrons = 30 - 75 % for  $P_{el} > 0.4$  GeV/c.

2) We then selected 4-prong events of the following type:

$$e^+e^- \rightarrow e^+\pi^+\pi^-\pi^- + \text{nothing else in the detector} + \text{missing mass} > 0.9 \text{ GeV} \quad (2)$$

We found 40 events of this type. The missing mass cut removes events of the reaction  $ee \rightarrow eeuu$ .

3) These events show a remarkable kinematic characteristic, as can be seen in Fig. 16: The invariant mass of the three-pion system is "low", the electron spectrum is "hard" and there is no correlation between the electron momentum and the  $3\pi$ -mass. This is expected for the reaction

$$e^+e^- \rightarrow \tau^+\tau^- \rightarrow e\nu\nu + \pi\pi\pi\nu. \quad (3a)$$

4) As a next step we check whether we really do see reaction (3a). For this purpose we split the events into samples where mass and momentum of the  $3\pi$ -system are consistent with reaction (3a) or inconsistent. In Fig. 17 we compare the  $\pi^+\pi^-$ -mass distribution to the expected punch through for these two samples. In the consistent sample (Fig. 17a) we find a significant excess of events and a clear  $\rho$ -peak. The inconsistent sample shows no  $\rho$  and can quantitatively be accounted for by the expected punch through. We conclude that in reaction (3a) we see a true signal of the channel

$$e^+e^- \rightarrow \tau^+\tau^- \rightarrow e\nu\nu + \rho^0\pi\nu. \quad (3b)$$

Since the electron events are clearly associated with a  $\rho^0$ -signal (consistent with 100 %  $\rho^0$ ) we investigate those events further having a  $\pi^+\pi^-$ -mass within the  $\rho^0$ -mass (0.70 - 0.84 GeV/c<sup>2</sup>). There are 23 events in this channel.

5) Can the events of reaction 3b also be explained by charm production? First we check that the 3 tracks besides the electron do not make up a charmed meson ( $D^+$  or  $F^+$ ). When calculating invariant masses with K-masses assigned to appropriate tracks we do not find a peak or even events at the corresponding resonance masses. Secondly, in Fig. 18 we compare the momentum spectrum of electrons from our reaction 3b with the inclusive electron spectrum observed by the DASP detector in general multiprong<sup>26</sup>. The dashed curve in Fig. 18 (only the shape is relevant) shows an eye-ball interpolation to the DASP spectrum, weighted with our momentum dependent efficiency. It is evident that the electrons from our reaction 3b are much harder. On the other hand, the electrons from reaction 3b agree with the spectrum expected from  $\tau$  decay (curve in Fig. 18). Finally we estimate the maximum possible contributions to reaction 3b from charm-pair production. In order to contribute to reaction 3b one charm meson has to decay into an electron and neutral particles, and the other has to decay into 3 charged particles plus at least one unobserved neutral particle. For the neutral particle we can exclude  $\pi^0$  since our overall detection efficiency for showers from a  $\pi^0$  is  $\sim 85\%$ . From the observed events consistent with  $e^+e^- \rightarrow e\pi^+\pi^-\pi^0$  and showers we conclude that less than two events can come from this charm decay. We also can exclude the possibility that the neutral particle is a  $K^0$  escaping detection. Combining the known decay branching ratios<sup>27</sup>  $D^+ \rightarrow L^+e^+\pi^0$  and  $D^+ \rightarrow \pi^+\pi^+\pi^-K^0$  we find that less than 10% of the yield in reaction 3b can be due to this source. In summary our data do not support an explanation by charm, nor do we expect charm production to account for the observed events. We thus continue to analyze the final state  $e\pi\pi$  as coming entirely from  $\tau$ -production.

6) Spin parity assignment: A three-pion state from  $\tau$ -decay must be in  $J^P = 1^P$  or  $0^-$ . A preliminary analysis of the Dalitz plot density distribution shows that both of these  $J^P$ -states are consistent with the data. Other  $J^P$ -states like  $1^-$ ,  $2^+$ , and  $2^-$  are significantly less consistent with the data.

7) We have already made sure that our signal is kinematically consistent with reaction (3a). Now we want to check whether the momentum distribution of the  $3\pi$ -system agrees with what is expected for a "two-body" decay  $\tau \rightarrow (3\pi) + \nu$ . For a given laboratory energy  $E_\tau$  of the  $\tau$  and a fixed mass  $M_{3\pi}$  of the  $3\pi$ -system the laboratory momentum  $P_{3\pi}^L$  has a uniform distribution between the limits  $P_{\min}(E_\tau, M_{3\pi})$  and  $P_{\max}(E_\tau, M_{3\pi})$ . These limits, however, are different for any  $E_\tau (= E_{\text{beam}})$  and  $M_{3\pi}$  (measured for each event). The quantity

$$U = \frac{P_{3\pi}^L - P_{\min}}{P_{\max} - P_{\min}}$$

is uniformly distributed between 0 and 1.

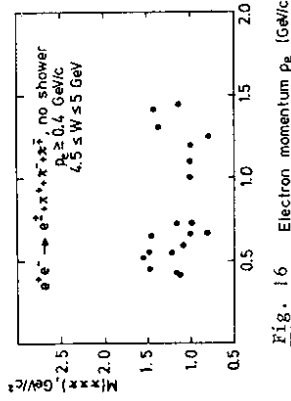


Fig. 16 Electron momentum  $P_e$  [GeV/c]

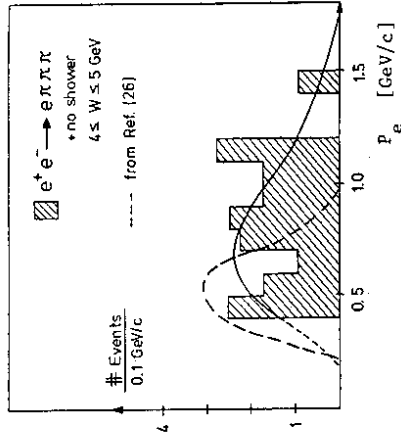


Fig. 18 Electron momentum distribution, not corrected for efficiency, and  $h \rightarrow e$  punch through subtracted. The broken line shows the shape for 'charm' electrons, derived from Ref. 26. The solid line is for  $\tau \rightarrow e\nu\nu$ . Both curves are multiplied by our momentum dependent electron efficiency.

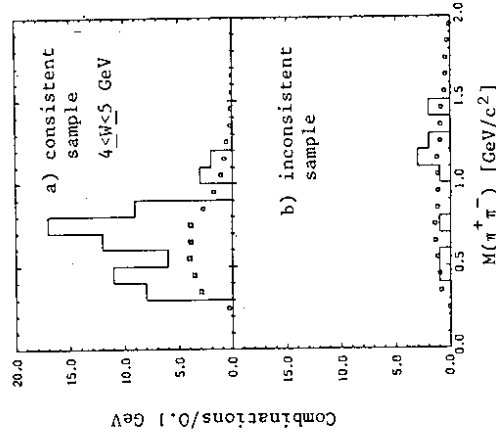


Fig. 17  $M(\pi^+\pi^-)$  for events which are

- a) kinematically consistent
- b) kinematically inconsistent with reaction 3a.

□ Background from  $h \rightarrow e$  punch through

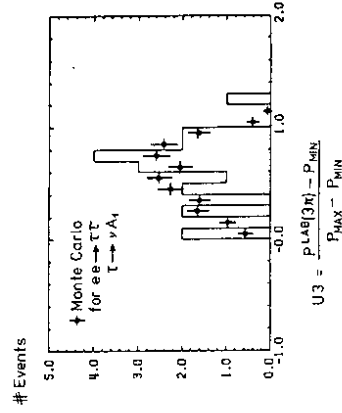


Fig. 19  $3\pi$  momentum, normalized to the kinematic range of a  $\tau$ -decay.

however, will be uniform again between 0 and 1, apart from acceptance and resolution effects. In Fig. 19 we compare the experimental distribution of  $U$  to the expectation for a two-body decay after imposing the detector acceptance onto Monte-Carlo events.

We note a good agreement between expectation and observation. In these calculations we used a massless neutrino and a  $\tau$ -mass of 1.9 GeV.

8) A further kinematic implication of reaction (3a) is the correlation between the direction of the electron and the  $3\pi$ -system, from the Lorentz boost. In Fig. 20 we show the cosine of the opening angle between these two vectors. Obviously, the back to back alignment gets stronger with growing beam energy. It also checks with the expectation we find from simulated events.

9) Now we turn to the question whether the data on the  $\rho\pi$ -system gives evidence for an  $A_1$ -meson. In Fig. 21 we show the  $3\pi$ -mass distribution for events having a  $p$ -combination (Fig. 21a) and those without (Fig. 21b). In Fig. 21a we note:

- a) a clear peak at  $M = 1.1$  GeV, with a width of  $\Gamma \approx 250$  MeV,
- b) virtually no events outside the  $A_1$  (there is no cut on the  $3\pi$ -mass!),
- c) the calculated background from punch through ( $h \rightarrow e$ ) makes up for  $< 20\%$  of the signal and has a clearly different shape.

In Fig. 21b we note

- a) no peak in the mass spectrum,
- b) the observed events can be quantitatively accounted for by the calculated  $h \rightarrow e$  punch-through background, i. e. we have no  $e\pi\pi\pi$  signal in events with no  $\pi\pi$ -mass in the  $\rho$  band.

The shape of the peak in Fig. 21a agrees with the shape of the  $J^P = 1^+ s$ -wave of the  $\rho\pi$ -system from a recent  $A_1$ -analysis in the reaction<sup>28</sup>  
 $\pi^+ p \rightarrow \pi^+ \pi^+ \pi^- \pi^+$   
 does not agree with the mass spectrum expected<sup>29</sup> for the decay

$$\tau \rightarrow \nu\rho\pi, \quad (\rho\pi) \text{ being non resonant}$$

as shown in Fig. 21a. The normalization of the  $\rho\pi$  curve is such that it shows an absolute upper limit for  $\tau$  decaying into this final state without enhancing effects like resonances. The data shows a clear excess of events over this upper limit in the  $A_1$ -mass region. We therefore conclude that the entire signal we see in reaction (3b) is consistent with and strongly suggestive for the reaction

$$e^+ e^- \rightarrow \tau\tau \rightarrow e\nu\nu + A_1\nu. \quad (3c)$$

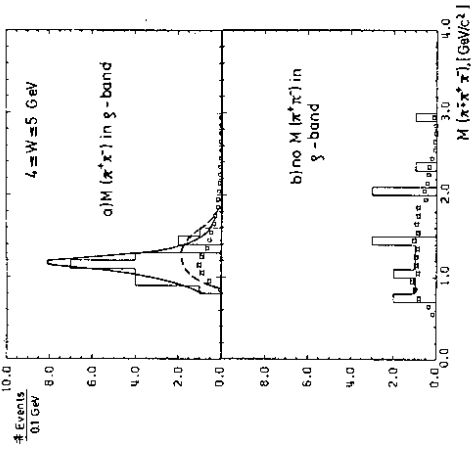


Fig. 21

$M(\pi^+ \pi^- \pi^-)$  from reaction 3a.

- Background from  $h \rightarrow e$  punch through.
- Theor. estimate (upper limit) on  $\tau \rightarrow \rho\nu\pi$  (nonresonant); Kawamoto, Kek, Sanda (private communication).

—  $1^+$  ( $\rho\pi$ ), s-wave, 15 GeV  $\pi^+ p \rightarrow \pi^+ \pi^+ \pi^-$  (Columbia, 32" HBC, SLAC)  
 $M = 1152 \pm 9, \Gamma = 264 \pm 11$  (Ref. 28).

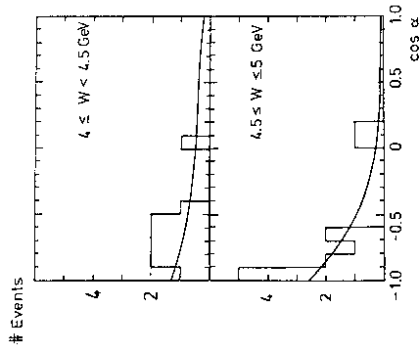


Fig. 20

Collinearity angle

$$\alpha = (\vec{e}, 3\vec{\pi}).$$

The curve is from a Monte-Carlo simulation of reaction 3c.

All these tests end up in favour of reactions (3a - 3c). We therefore interpret our data in terms of these reactions and determine the following results.

1) Cross Section and Branching Ratios:

W [GeV]	observed events	expected punch-through	cross section a) $B(\text{e}\nu\nu)\times B(\rho^0\pi\nu)$ pb	b) $B(\nu A_1)$	c)
3.6	0	< 1	-		
4 - 4.5	11	2.5	$37 \pm 11$	$0.0077 \pm 0.0023$	$0.11 \pm 0.04$ $\pm 30\% \text{ syst.}$
4.5 - 5.0	12	2	$60 \pm 17$	$0.010 \pm 0.003$	

- a) At present there is an additional systematic uncertainty of 30 % in the acceptance used.
- b) Using a  $\tau$ -mass of 1.9 GeV in calculating  $\sigma(\text{e}\bar{\text{e}} \rightarrow \tau\bar{\tau})$ .
- c) Using  $B(\tau \rightarrow \text{e}\nu) = 0.16$ .

2) Neutrino mass: In the semihadronic decay  $\tau \rightarrow \nu\pi\pi$  the  $\tau$ -neutrino is the only missing particle. If the  $\tau$ -mass is known then for each event we can calculate an upper limit for the neutrino mass to be consistent with the measured kinematic quantities. For  $M_1 = 1.9 \text{ GeV}/c^2$  11 events require an upper limit of less than the 540 MeV/c<sup>2</sup> which was reported in section A, and all of the 23 events are consistent with an upper limit of 300 MeV/c<sup>2</sup>.

In summary, we have found

- (1) clear evidence for the decay  $\tau^{\pm} \rightarrow \rho\pi^{\mp}\nu$
- (2) that this decay is entirely consistent with and strongly suggestive for the decay  $\tau \rightarrow A_1\nu$ .

The predicted branching ratio<sup>24</sup> of 7 % for  $\tau \rightarrow A_1\nu$  is consistent with our result.

I would like to thank all my colleagues who helped in preparing this talk.

REFERENCES

- (1) PLUTO Collaboration J. Burmester et al., Phys. Lett. 66B (1977) 395; and further references given there.
- (2) For details see A. Bäcker, Thesis, GHS Siegen, Germany 1977; DESY internal report F33-77/03 (1977).
- (3) We use a  $\tau$ -mass of 1.9 GeV/c<sup>2</sup> in calculating  $R(\tau)$ .
- (4) T.W. Appelquist and H. Georgi, Phys. Rev. D8 (1973) 4000; A. Zee, Phys. Rev. D8 (1973) 4038.
- (5) E. Eichten et al., Phys. Rev. Lett. 36 (1976) 500; E. Eichten, K. Lane, Phys. Rev. Lett. 37 (1976) 477.
- (6) S. Yamada, invited talk at this conference, to be published in the proceedings.
- (7) J. Siegrist et al., Phys. Rev. Lett. 36 (1976) 700.
- (8) Ch. Berger et al., DESY report 77/47 (1977), to be published in Phys. Letters.
- (9) PLUTO Collaboration J. Burmester et al., Phys. Lett. 67B (1977) 367, for  $K^0$ ; PLUTO Collaboration J. Burmester et al., Phys. Lett. 68B (1977) 283, for  $J/\psi$ .
- (10) G.G. Hanson, Talk given at the XVIIIth Int. Conf. on High Energy Physics Tbilisi, USSR (1976); SLAC-PUB-1814 (1976).
- (11) DASP Collaboration R. Brandelik et al., Phys. Lett. 67B (1977) 358.
- (12) S. Yamada, invited talk at this conference; to be published in the proceedings.
- (13) C. Rosenzweig, Phys. Rev. Lett. 36 (1976) 697; M. Bander et al., Phys. Rev. Lett. 36 (1976) 695; A. de Rujula et al., Phys. Rev. Lett. 38 (1977) 317.
- (14) T.F. Walsh, DESY report 76/13 (1976); R. Köbeler, G. Schierholz and G. Kramer, Phys. Lett. 65B (1976) 441.
- (15) S. Okubo, Phys. Lett. 5 (1963) 105; G. Zweig, CERN report TH 401 (1964) 412; J. Iizuka, K. Okada and O Shito, Prog. Theo. Phys. 35 (1966) 1061.
- (16) W. Bartel et al., DESY report 76/65 (1976); DASP Collaboration W. Braunschweig et al., Phys. Lett. 67B (1977) 243.

- (17) R.N. Cahn, M.S. Chanowitz, Phys. Lett. 59B (1975) 277;  
T.F. Walsh, Nuovo Cimento Lett. 14 (1975) 290;  
H. Barari, Phys. Lett. 60B (1976) 172;  
A. Kazi, G. Kramer, D.H. Schiller, Acta Phys. Austr. 45 (1976)  
65 and 45 (1976) 195;  
Nuovo Cimento Lett. 15 (1976) 120.
- (18a) PLUTO Collaboration J. Burmester et al., DESY report 77/50 (1977);  
to be published in Physics Letters.
- (18b) PLUTO Collaboration G. Alexander et al., DESY report 77/72 (1977);  
submitted for publication.
- (19) M.L. Perl et al., Phys. Rev. Lett. 35 (1975) 1489.
- (20) M.L. Perl et al., Phys. Lett. 63B (1976) 466;  
G.J. Feldman et al., Phys. Rev. Lett. 38 (1976) 117;  
M. Cavalli-Sforza et al., Phys. Rev. Lett. 36 (1976) 588;  
H. Meyer, Proceedings of the Orbis Scientiae, Coral Gables (1977);  
DESY Report 77/19 (1977);  
PLUTO Collaboration J. Burmester et al., Phys. Lett. 68B (1977)  
.297;  
PLUTO Collaboration J. Burmester et al., Phys. Lett. 68B (1977)  
301.  
DASP Collaboration R. Braudelik et al., Phys. Lett. 70B (1977) 125.
- (21) G. Flügge, Proceedings of the Vth International Conf. on Experi-  
mental Meson Spectroscopy, North Eastern University, Boston (April  
1977) and DESY 77/35 (1977);  
M.L. Perl, Proceedings of the XII Rencontre de Moriond, France (1977)  
and SLAC report SLAC-PUB-1923 (1977);  
M.L. Perl, invited talk at this conference;  
U. Thimm, Proceedings of the EPS European Conference on Particle  
Physics, Budapest (1977) and DESY report 77/52 (1977).
- (22) See ref. 20, papers 5 and 6.
- (23) F. Gutbrod, Z.J. Rek, DESY report 77/45 (1977).
- (24) Y.S. Tsai, Phys. Rev. D4 (1971) 2821;  
H.B. Thacker, J.J. Sakurai, Phys. Lett. 36B (1971) 103.
- (25) T.F. Walsh, invited talk at this conference.
- (26) See ref. 20, paper 7.
- (27) G.J. Feldman and M.L. Perl, SLAC report SLAC-PUB-1972 (1977).
- (28) C.V. Cautis, Thesis University of Columbia 1977;  
R1097, CU327, Nevis 221.
- (29) N. Kawamoto, Z.J. Rek and A. Sanda, private communication.